Identification of the $2^+_{1,\mathrm{ms}}$ mixed-symmetry state in ^{136}Ce

T. Ahn,[1,2,3,*] G. Rainovski,[3,4] N. Pietralla,[3] L. Coquard,[3] T. Möller,[3] A. Costin,[2] R. V. F. Janssens,[5] C. J. Lister,[5] M. P. Carpenter,[5] and S. Zhu[5]

[1]*Wright Nuclear Structure Laboratory, Yale University, New Haven, Connecticut 06520, USA*
[2]*Department of Physics and Astronomy, Stony Brook University, Stony Brook, New York 11794-3800, USA*
[3]*Institut für Kernphysik, Technische Universität Darmstadt, 64289, Darmstadt, Germany*
[4]*Faculty of Physics, St. Kliment Ohridski University of Sofia, Sofia 1164, Bulgaria*
[5]*Argonne National Laboratory, 700 South Cass Avenue, Argonne, Illinois 60439, USA*

(Received 23 April 2012; published 3 July 2012)

The evolution of the one-quadrupole phonon mixed-symmetry state is important for understanding the role of the quadrupole proton-neutron interaction in the valence shell. To study the evolution of the $2^+_{1,\mathrm{ms}}$ mixed-symmetry state in the $N = 78$ isotones above $Z = 50$, a Coulomb excitation measurement was performed to identify the $2^+_{1,\mathrm{ms}}$ state in ^{136}Ce by measuring absolute transition strengths. The $2^+_{1,\mathrm{ms}}$ state was found to be predominantly concentrated in the 2^+_4 state of this nucleus. The simple picture of shell stabilization given to account for the fragmentation of the strength observed in ^{138}Ce does not seem to apply to ^{136}Ce.

DOI: 10.1103/PhysRevC.86.014303 PACS number(s): 21.10.Re, 23.20.Gq, 25.70.De, 27.60.+j

I. INTRODUCTION

Atomic nuclei display a number of collective phenomena. Two of the best-known examples of collective motion are rotations of a deformed nucleus and surface vibrations of a spherical one. The quanta of these types of collective motion are represented by bosons in the Interacting Boson Model (IBM) [1]. In the IBM, the bosons are also interpreted as a superposition of pairs of nucleons outside of a closed shell. In the proton-neutron version of the IBM, the Interacting Boson Model-2 (IBM-2) [1,2], proton bosons are distinct from neutron bosons. This leads to a new type of excitation called a mixed-symmetry state (MSS), interpreted geometrically as an excitation where protons and neutrons are moving out of phase with respect to each other. Because of this out-of-phase motion, MSSs are sensitive to the restoring force between the proton and neutron excitations and are, thus, sensitive to the proton-neutron interaction in the valence shell. Therefore, they are important sources of information on the details of the effective residual interactions between valence nucleons.

In the IBM-2, the definition of MSSs is formalized in terms of the bosonic F-spin symmetry [2]. Fully symmetric states (FSSs) have the maximum value of F spin, $F_{\max} = (N_\pi + N_\nu)/2$, where N_π and N_ν are the number of proton and neutron bosons, respectively. MSSs are associated with $F = F_{\max} - 1$. F spin for proton and neutron bosons is analogous to isospin for protons and neutrons. In vibrational nuclei, the fundamental MSS is the one-quadrupole phonon $2^+_{1,\mathrm{ms}}$ state [2], which is the lowest-lying isovector quadrupole excitation in the valence shell [3]. Because of its isovector nature, the $2^+_{1,\mathrm{ms}}$ state decays with a strong $M1$ transition to the one-phonon FSS and with a weak $E2$ transition to the ground state. This unique decay serves as an experimental fingerprint for the $2^+_{1,\mathrm{ms}}$ state.

A large number of one-quadrupole phonon ($2^+_{1,\mathrm{ms}}$) MSSs have been identified in the mass $A = 90$ and $A = 130$ regions through the measurement of absolute electromagnetic transition strengths [4]. In the last several years, the number of identified MSSs in the mass $A = 130$ region has grown substantially. By using projectile Coulomb excitation reactions and the Gammasphere array at Argonne National Laboratory, the one-phonon MSSs were identified in several stable nuclei, for example, ^{138}Ce [5] and ^{130,132,134}Xe [6–8]. Moreover, the $2^+_{1,\mathrm{ms}}$ state of the $N = 80$ isotone ^{132}Te has been predicted [6] and very recently identified [9]. These experimental results demonstrate not only a new experimental approach for the investigation of MSSs, but also show that the underlying microscopic structure of the nucleus can have a strong influence on the properties of these states. In fact, for collective vibrational nuclei, the single-particle structure of the wave functions can be the most important factor for preserving or fragmenting the MSSs. For example, the observed fragmentation of the one-phonon MSS in ^{138}Ce is attributed to the lack of shell stabilization at the proton $g_{7/2}$ subshell closure [5].

The evolution of the MSSs along the $N = 80$ isotones has inspired extended microscopic calculations of their structure within the framework of the quasiparticle-phonon model (QPM) [10] as well as in large-scale shell-model calculations [11]. The QPM calculations have suggested that the splitting of the $M1$ strength in ^{138}Ce is a genuine shell effect caused by the specific shell structure and pairing correlations. However, the large-scale shell-model calculations did not exhibit such splitting. Alternatively, the latter shell-model calculations did point to the importance of tuning the pairing strength to reproduce the $M1$ transition strengths in the $N = 80$ isotones. Although these microscopic models agree that the stability of MSSs is related to the single-particle structure and aspects of the nucleon-nucleon interaction, the generic nature of the shell stabilization is not yet fully understood. Progress in this understanding will require MSSs in ^{140}Nd and ^{136}Ce to be firmly identified on the basis of measured absolute $M1$

*Current address: National Superconducting Cyclotron Laboratory, Michigan State University, 640 South Shaw Lane, East Lansing, MI 48824.

transition strengths. The properties of the one-phonon MSS in ^{140}Nd will reveal whether the shell stabilization mechanism is present when the proton excitations are developed predominantly in the $d_{5/2}$ subshell. The properties of the one-phonon MSS in ^{136}Ce will show to what extent the mechanism is influenced by neutron degrees of freedom. One of the aims of the present study is to investigate the latter problem by providing a firm identification and a quantitative study of the properties of the one-phonon $2^+_{1,\mathrm{ms}}$ MSS of ^{136}Ce.

The firm identification of the one-phonon MSS of ^{136}Ce will also help reveal the evolution of the MSSs in the $N = 78$ isotones. This evolution is interesting because it allows an extraction of the local strength of the proton-neutron quadrupole interaction by using the properties of both symmetric and antisymmetric one-phonon states as described in Ref. [12]. In fact, this procedure was already applied for the $N = 80$ isotones [6] and for the xenon isotopes [8]. Surprisingly, the values obtained differ significantly (by about 10%) while a more constant behavior is expected when the proton-neutron quadrupole interaction is derived from the properties of the symmetric states only [12]. The observed discrepancy is argued in Ref. [8] to be attributable to limited experimental sensitivity, which does not allow higher-lying fragments of MSSs in lighter xenon isotopes to be identified. However, the direct comparison between the derived values for the proton-neutron interaction in the xenon chain and in the $N = 80$ isotonic chain is not entirely consistent because the latter nuclei are vibrational in character while the former exhibit a transition from vibrational [U(5)-like] to γ-soft [O(6)-like] structure. Such structural changes may violate the assumption on which the procedure for extracting the local proton-neutron quadrupole interaction is based [12]. Therefore, it seems more appropriate to investigate the possible variations in the local proton-neutron quadrupole interaction by comparing its values for the $N = 80$ [6] and $N = 78$ isotonic chains.

Candidates for the $2^+_{1,\mathrm{ms}}$ state of ^{136}Ce have been proposed from a measurement of $E2/M1$ multipole mixing ratios [13]. It was suggested that there is a nearly equal fragmentation of this $2^+_{1,\mathrm{ms}}$ state into the 2^+_3 and 2^+_4 levels. In the present study, we report on the firm identification of the one-phonon $2^+_{1,\mathrm{ms}}$ state based on the measured $B(M1)$ strength distribution. The experimental results clearly demonstrate that the $2^+_{1,\mathrm{ms}}$ level is a single isolated state, which, as shown below, indicates that the neutron degrees of freedom play an important role in the mechanism of shell stabilization. The value of the local proton-neutron quadrupole interaction obtained from the properties of both symmetric and antisymmetric one-phonon states in the $N = 78$ isotones is significantly smaller than that in the $N = 80$ isotones, again underlying the importance of the neutron degree of freedom for forming the MSSs.

II. EXPERIMENT AND RESULTS

A Coulomb excitation experiment in inverse kinematics was carried out to measure electromagnetic transition strengths in ^{136}Ce. The experiment was performed at the Argonne National Laboratory, where a beam of ^{136}Ce was accelerated to an energy of 475 MeV using the ATLAS superconducting linac.

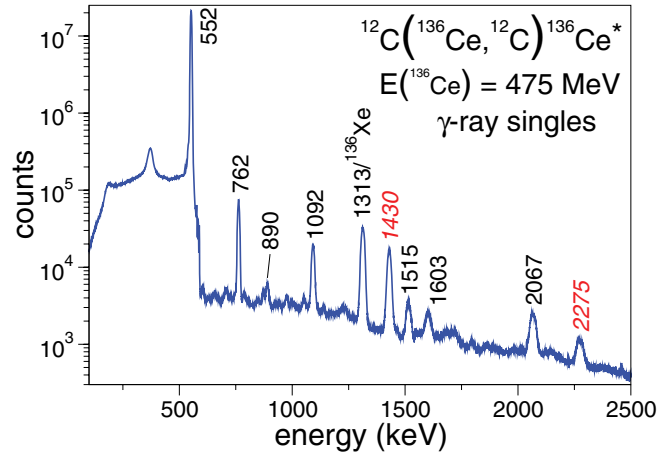

FIG. 1. (Color online) Doppler-corrected singles spectrum from Coulomb excitation of ^{136}Ce. New transitions are shown in oblique (red color) type. The 1313-keV peak corresponds to the $2^+_1 \rightarrow 0^+_1$ transition of ^{136}Xe, which appears as a beam contaminant.

This beam energy corresponds to 82% of the Coulomb barrier and the beam had an intensity of 1 pnA. The beam impinged upon a natural carbon target with an effective thickness of 1.2 mg/cm^2. The γ rays emitted from Coulomb-excited nuclei were detected with the Gammasphere array [14,15], which consisted of 101 Compton-suppressed high-purity Ge detectors. The trigger for an event was the detection of a single Compton-suppressed γ ray. Higher fold coincidence events were recorded as well. All events were written in list mode to tape and a total of 8.4×10^8 events, of which 1.4×10^7 were of multiplicity two or higher, were recorded over a period of 38 h. All the γ-ray energies were Doppler corrected according to the observation angle with respect to the beam direction. A Doppler-corrected spectrum for the sum of all γ rays detected in the experiment is given in Fig. 1.

A level scheme showing all observed transitions and corresponding levels is presented in Fig. 2. Two new levels and their corresponding decay transitions have been observed. These are a tentatively assigned (3^-) state at 1982 keV and a level at 2275 keV with a tentative spin and parity of (2^+). The placement of these levels was determined using the available $\gamma\gamma$ coincidence data. A coincidence spectrum of a gate on the 552-keV $2^+_1 \rightarrow 0^+_1$ transition is found in Fig. 3. For the 1982-keV level, a ground-state decay is not observed, consistent with a spin larger than two. This observation together with the sizable yield strongly suggest that the 1982-keV state is populated via a one-step electric octupole excitation providing a tentative spin and parity assignment of (3^-). In addition, as discussed below, the excitation energy is in line with that of 3^- levels in neighboring nuclei. In contrast, for the 2275-keV level, a strong ground-state decay was observed, as would be the case for the tentatively proposed (2^+) assignment. There were a number of additional transitions observed in the coincidence spectra, but these could not be definitively placed in the level scheme owing to insufficient coincidence data. The energies of these observed transitions are 873(1), 1139(1), 1750(1), 1796(1), and 2369(5) keV. It has to be noted that

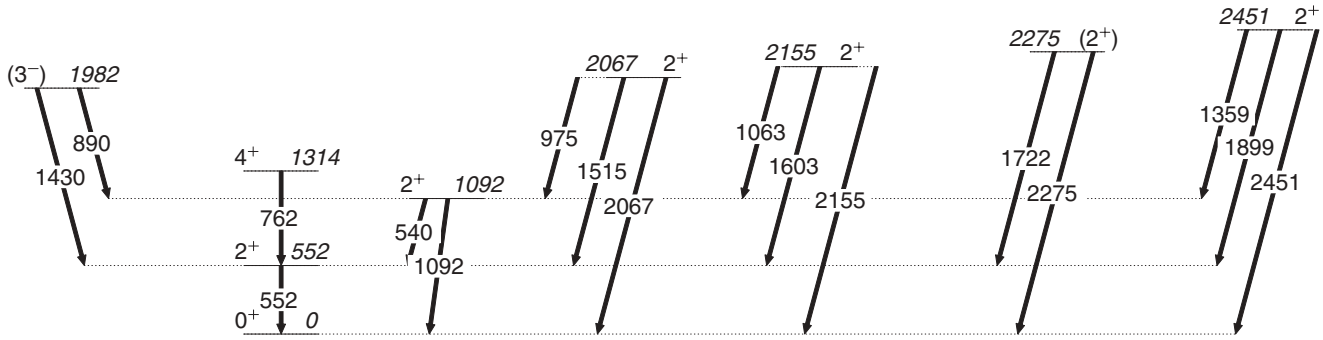

FIG. 2. Level scheme with all transitions and their corresponding levels observed in the present Coulomb excitation of ^{136}Ce.

the intensities of these γ rays are smaller than 10^{-4} with respect to the intensity of the $2^+_1 \rightarrow 0^+_1$ transition. Therefore, they do not influence substantially the relative population of the observed states. The remaining observed transitions and measured intensities are given in Table I.

From the observed total γ yield and knowledge of the low-lying structure of ^{136}Ce, cross sections relative to the 2^+_1 state were deduced. Absolute cross sections were calculated from the knowledge of the $0^+_1 \rightarrow 2^+_1$, $E2$ transition strength. The multistep Coulomb excitation code CLX [17,18] based on the program by Winther and de Boer [19] was used to determine the transition matrix elements for the observed transitions. We started by using electromagnetic matrix elements calculated by assuming that the population of all states came solely from one-step excitations (cf. Ref. [20]). From these initial matrix elements, we calculated the decay strengths of all observed γ transitions using the measured branching ratios taken from Ref. [13]. The set of matrix elements obtained this way was then used for a full multistep Coulomb excitation calculation. The matrix elements were then tuned to reproduce the yields observed in the experiment while keeping the agreement with the measured branching ratios and multipole mixing ratios. This procedure was iterated until convergence was reached within experimental uncertainties. Because the diagonal matrix elements, representing static quadrupole moments, were unknown, calculations were done varying these moments between the rotational limits and were accounted for in the overall uncertainty. All deduced transition strengths are given in Table I. In the cases of unknown $E2/M1$ multipole mixing ratios, we report upper limits for the decay strengths of each multipolarity by separately assuming all strengths being attributable to either a pure $E2$ or a pure $M1$ transition alone. The measured $E2$ and $M1$ transition strengths in ^{136}Ce are plotted in Fig. 4. From the relative population of the (3^-) state at 1982 keV we were able to determine the $B(E3)\uparrow$ value, assuming that this state is populated entirely through a one-step $E3$ excitation. The static quadrupole moment of this (3^-) state was set to zero. The $M(E3; 0^+_1 \rightarrow 3^-)$ matrix element was then varied to reproduce the observed yield. This results in a value $B(E3)\uparrow = 0.19(3)\ e^2\,\mathrm{b}^3$. This value is comparable to the one measured in ^{138}Ce ($B(E3)\uparrow = 0.163(9)\ e^2\,\mathrm{b}^3$ [5]). Moreover, from the detection limit at 1982 keV, we have deduced that the upper limit for the intensity of the $E3$ ground-state decay is $<10^{-5}$ with respect to the intensity of the $2^+_1 \rightarrow 0^+_1$ transition. This results in lower limits $B(E1; 3^- \rightarrow 2^+_1) > 6.4 \times 10^{-5}$ W.u. and $B(E1; 3^- \rightarrow 2^+_2) > 2.6 \times 10^{-5}$W.u.. These values are in agreement with our initial assumption that the $E1$ transitions involved in two-step processes do not contribute to the observed Coulomb excitation yield of the (3^-) state at 1982 keV.

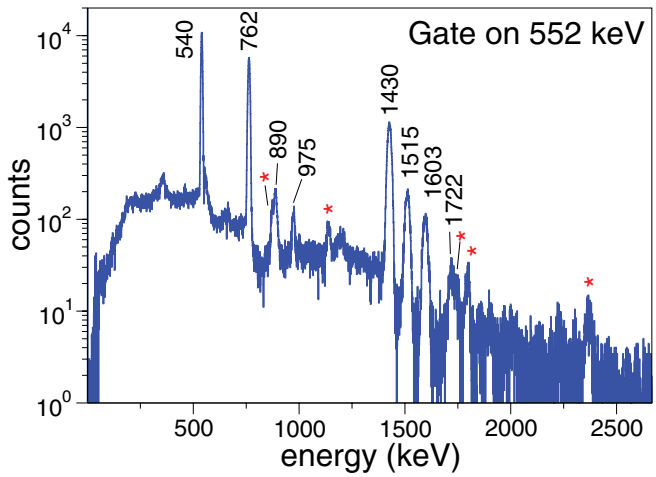

FIG. 3. (Color online) A spectrum showing the transitions in coincidences with the 552-keV $2^+_1 \rightarrow 0^+_1$ transition. Asterisks indicate transitions that could not be placed in the level scheme (see text).

III. DISCUSSION

Of the measured transition strengths, the 2^+_4 state has the largest $B(M1; 2^+_i \rightarrow 2^+_1)$ value of 0.16(3) μ^2_N and, thus, is assigned as the main fragment of the $2^+_{1,ms}$ state of ^{136}Ce. The observed lack of the fragmentation of the $2^+_{1,ms}$ state differs from what was previously suggested on the basis of the observed multipole mixing ratios [13]. This situation clearly demonstrates that, for safe MSS assignments, the absolute $M1$ strength plays a crucial role. The multipole mixing ratios provide important experimental information and may hint at the existence of MSS, but they are not sufficient for a safe assignment or a quantitative analysis.

The fragmentation of the one-phonon MSS of ^{136}Ce is much smaller than the one observed in ^{138}Ce [5]. This clearly indicates that the lack of shell stabilization suggested in ^{138}Ce

TABLE I. Energy of the state E_{level}, spin and parity J^π, energy of the γ-ray transition E_γ, spin and parity of the final state J^π_{final}, relative γ-ray intensity I_γ, multipole mixing ratio δ (taken from Ref. [13]), and transition strengths $B(E2)$ and $B(M1)$ for all transitions in ^{136}Ce measured in the present work.

E_{level}	J^π	E_γ	J^π_{final}	I_γ	δ	Transition strength	
(keV)	(keV)					$B(E2)$ (W.u.)	$B(M1)$ (μ_N^2)
552	2_1^+	552	0_1^+	1000(4)		39(4)[a]	
1092	2_2^+	1092	0_1^+	2.39(4)		0.55(9)	
		540	2_1^+	6.5(3)	$-4.7(7)$[b]	48(7)	0.0010(9)
1314	4_1^+	762	2_1^+	5.5(1)		56(10)[c]	
1982	(3^-)	(1982)[d]	0_1^+	$<10^{-2}$		$B(E3)\uparrow = 0.19(3)e^2\,\text{b}^3$	
		1430	2_1^+	3.4(1)		$B(E1) > 6.4\times10^{-5}$ W.u.[e]	
		890	2_2^+	0.33(1)		$B(E1) > 2.6\times10^{-5}$ W.u.[e]	
2067	2_3^+	2067	0_1^+	0.74(2)		1.2(6)	
		1515	2_1^+	0.59(1)	0.46(8)[b]	0.79(4)	0.025(2)
		975	2_2^+	0.103(4)		$\leqslant$7(2)[f]	$\leqslant$0.02(1)[g]
2155	2_4^+	2155	0_1^+	0.035(5)		0.56(3)	
		1603	2_1^+	0.41(2)	$-0.41(8)$[b]	4.0(3)	0.16(3)
		1063	2_2^+	0.023(4)		$\leqslant$11(2)[f]	$\leqslant$0.036(7)[g]
2275	(2^+)	2275	0_1^+	0.30(1)		0.57(4)	
		1722	2_1^+	0.086(4)		$\leqslant$0.6(2)[f]	$\leqslant$0.0052(4)[g]
2451	$2^+_{(6)}$	2451	0_1^+	0.029(9)		0.26(3)	
		1899	2_1^+	0.030(2)		$\leqslant$0.9(2)[f]	$\leqslant$0.009(3)[g]
		1359	2_2^+	0.040(12)		$\leqslant$6(2)[f]	$\leqslant$0.04(2)[g]

[a]Value from Ref. [16].
[b]Values from Ref. [13].
[c]No $E4$ contribution is included in the population of the 4_1^+ state.
[d]This transition is not observed. The upper limit for its intensity is estimated from the detection limit.
[e]Estimated from the upper limit of the decay to the ground state and the observed branching ratio.
[f]Upper limit based on the assumption of a pure $E2$ transition.
[g]Upper limit based on the assumption of a pure $M1$ transition.

is not exhibited in ^{136}Ce. Using the two-state mixing scenario from Ref. [5], it can be shown that the small portion of the $M1$ strength distributed to the 2_3^+ state of ^{136}Ce leads to a mixing

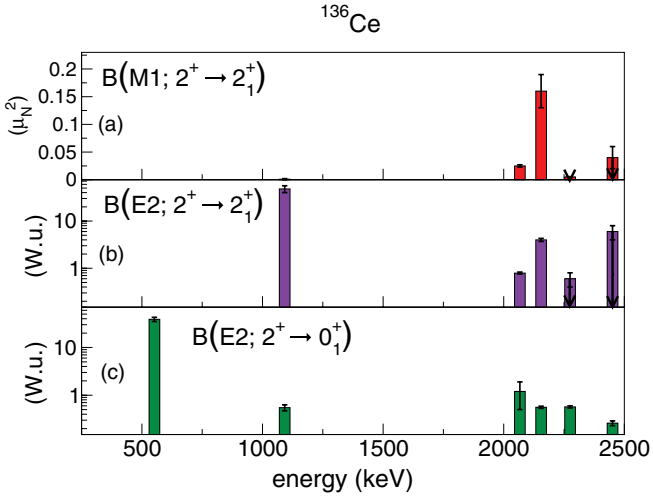

FIG. 4. (Color online) (a) $B(M1;2^+ \to 2_1^+)$, (b) $B(E2;2^+ \to 2_1^+)$, and (c) $B(E2;2^+ \to 0_1^+)$ transition strength distributions for all observed 2^+ states below 2.5 MeV in ^{136}Ce. Upper limits for transition strengths are denoted with arrows.

matrix element between the pure MSS and a nearby FSS of 20(3) keV. This value is a factor of 2 smaller than the one derived for ^{138}Ce. Apparently, the reason for this difference is related to the microscopic structure of the one-phonon states in these two isotopes. In ^{138}Ce, the fragmentation of the MSS is explained as owing to a lack of shell stabilization at the proton $g_{7/2}$ subshell. In fact, it was shown in the framework of the QPM that the mechanism is more complex [10]. Owing to the proton $g_{7/2}$ subshell, the lowest two-quasiparticle proton excitations are packed closely together, which leads to two collective 2^+ RPA states of isovector nature located above the first 2^+ RPA solution. This structure is preserved in the QPM solutions that describe the two fragments of the MSS in ^{138}Ce. This scenario implies that the two-quasiparticle proton energies are close in energy to the two-quasiparticle neutron energies. In ^{136}Ce, the proton single-particle structure is the same as in ^{138}Ce. However, the presence of two additional neutron holes apparently influences the energies of the two-quasiparticle neutron excitations in such a way that their relative position with respect to the two-quasiparticle proton ones changes. As a result, one of the 2^+ RPA solutions above the first 2^+ RPA one may lose its collective character as in the case of ^{136}Ba and ^{134}Xe [10]. Such a scenario leads to a purer one-phonon MSS for ^{136}Ce compared to the one of ^{138}Ce.

An indirect argument supporting this scenario may be the fragmentation of the $2^+_{1,ms}$ MSS of ^{134}Ba from which a mixing matrix element of 24(5) keV can be extracted [21], while the same matrix element for ^{136}Ba is <10 keV [5,22]. Again, owing to the relative change of the energy of the two-quasiparticle neutron configuration in ^{134}Ba with respect to the case of ^{136}Ba, there may be more 2^+ RPA solutions of isovector nature above the first 2^+ RPA solution which ultimately could lead to the observed fragmentation. It has to be stressed, however, that to understand the fragmentation of MSSs in the Ce-Ba region and confirm the validity of the qualitative arguments above, detailed QPM calculations are required for the $N = 78$ isotones. However, a direct experimental confirmation of the mechanism of shell stabilization in the $N = 80$ isotones, which is a phenomenon related to the proton structure, should be sought for by identifying the MSS in ^{140}Nd. Candidates for the $2^+_{1,ms}$ level have been proposed from measured multipole mixing ratios [23] and lifetime measurements with the Doppler-shift attenuation method (DSAM) [24]. However, the DSAM measurement did not obtain transition strengths for all possible fragments of the $2^+_{1,ms}$ state in ^{140}Nd, and this leaves open the issue about the generic nature of shell stabilization.

Along with the $2^+_{1,ms}$ state found here in ^{136}Ce, the $2^+_{1,ms}$ state has also been identified in ^{134}Ba [21,25] and ^{132}Xe [8], and candidates for fragments of the $2^+_{1,ms}$ state have been reported in ^{130}Te [26]. The transition strengths for these $N = 78$ nuclei are presented in Fig. 5. The data along the $N = 78$ isotonic chain suggest a smooth increase of the 2^+_{ms} excitation energy

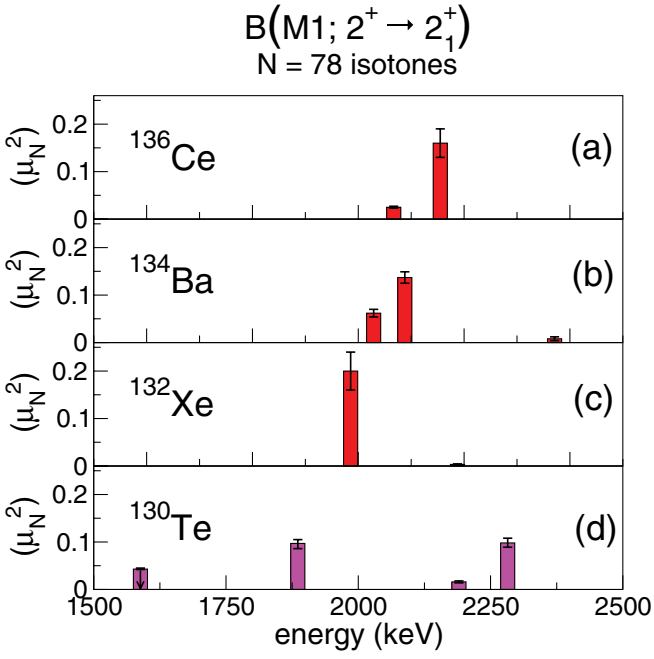

FIG. 5. (Color online) $M1$ transition strength distributions for the $N = 78$ isotones (a) ^{136}Ce, (b) ^{134}Ba, (c) ^{132}Xe, and (d) ^{130}Te. The transition strengths for ^{130}Te are the larger of two possible values owing to the two possible values of the multipole mixing ratio found for these transitions (see Ref. [26] for details).

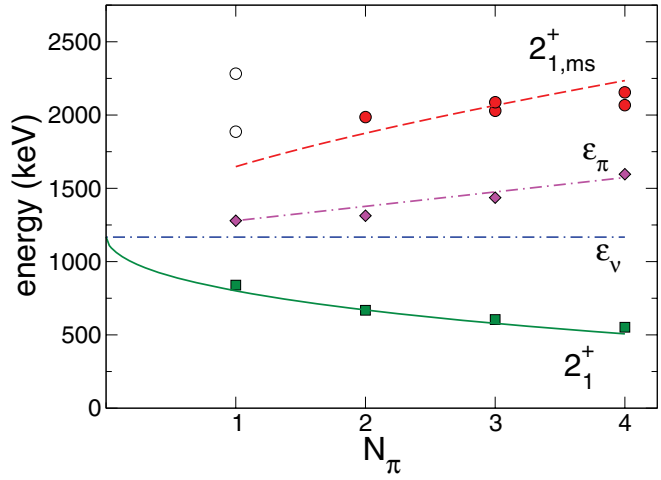

FIG. 6. (Color online) Simultaneous fit of the experimental energies of the 2^+_1 states (solid curve) and of the $B(M1)$-weighted average energies of the $2^+_{1,ms}$ states (dashed curve) in the $N = 78$ isotones. The experimental energies of the 2^+_1 levels and of the fragments of the $2^+_{1,ms}$ states are represented with solid squares and circles, respectively. The energies of the main fragments of the $2^+_{1,ms}$ state in ^{130}Te, which are not included in the fit shown, are represented with open circles. The dash-dotted lines labeled ε_π and ε_ν represent the unperturbed energies of the proton and the neutron state, respectively. The energies of the 2^+_1 states of the corresponding closed-shell $N = 82$ isotones are given as diamonds.

with increasing proton number, that is, with an increasing size of the valence space.

Figure 6 provides the excitation energies of the 2^+_1 and $2^+_{1,ms}$ states as a function of the proton boson number N_π in the $N = 78$ isotonic chain. It can be noted that the energy of the 2^+_1 level decreases as one moves to higher proton boson number N_π. At the same time, the energy of the $2^+_{1,ms}$ state or the average energy of the fragments of the $2^+_{1,ms}$ state, weighted by their $B(M1; 2^+_i \rightarrow 2^+_1)$ values, increases as the function of N_π. The only exception from this behavior is in the case of ^{130}Te, where the one-phonon MSS may be strongly fragmented [26] as some possible fragments appear at a relatively high energy (see Fig. 5).

In the simple two-state mixing scheme outlined in Refs. [6,12], the one-phonon 2^+_1 and the $2^+_{1,ms}$ states arise from the mixing of the fundamental proton and neutron 2^+ configurations. This mixing is caused by the proton-neutron quadrupole interaction which is parametrized as $V_{\pi\nu} = \beta\sqrt{N_\pi N_\nu}$ where $N_\pi(N_\nu)$ denote proton (neutron) pairs in the valence shell and β is a strength parameter [12]. For stable, even-even $N = 78$ isotones, $N_\nu = 2$ while N_π varies between 1 and 4 for the nuclei considered here (Fig. 6). This scheme was used to fit the splitting between the energies of the 2^+_1 states and the $B(M1)$-weighted average values for the energies of the $2^+_{1,ms}$ states. The approach to taking into account the $B(M1)$-weighted average values for the energies of the $2^+_{1,ms}$ states, instead of the energies of the main fragments, is motivated by the fact that the fragmentation of one-phonon MSS has a microscopic origin [10,11] which is outside the

framework of the simple two-state mixing model [12]. The one-phonon MSS of ^{130}Te was not included in the fit presented in Fig. 6 as the $M1$-average cannot be determined from the data because of the ambiguous values for the multipole mixing ratios. The unperturbed neutron energy, ε_ν, for the $N = 78$ isotonic chain was chosen as the energy of the 2_1^+ state of the $Z = 50$, semimagic nucleus ^{128}Sn [i.e., $\varepsilon_\nu(^{128}\mathrm{Sn}) = 1169$ keV]. The dependence of ε_π on proton number over the $N = 78$ isotonic sequence was taken into account by assuming that it follows the 2_1^+ energies in the nearby semimagic $N = 82$ isotopes (no valence neutrons; i.e., $N_\nu = 0$) (Fig. 6). Therefore, the unperturbed energy of the proton state was linearly parametrized by the expression $\varepsilon_\pi = a + b(N_\pi - 1)$ where a was chosen to be equal to the energy of the 2_1^+ state in the neutron closed-shell nucleus ^{134}Te [i.e., $a = E(2_1^+)(^{134}\mathrm{Te}) = 1279$ keV]. From the two-state mixing scheme, the resulting energies of the one-phonon 2^+ states (2_1^+ and $2_{1,\mathrm{ms}}^+$) can be expressed as

$$E(2_1^+, 2_{1,\mathrm{ms}}^+) = \frac{\varepsilon_\pi + \varepsilon_\nu}{2} \pm \sqrt{\frac{(\varepsilon_\pi - \varepsilon_\nu)^2}{4} + \beta^2 2N_\pi},$$

where $+$ $[-]$ applies to the $E(2_{1,\mathrm{ms}}^+)$ and $E(2_1^+)$ energies, respectively. The values of parameters b and β were derived simultaneously from a least-squares fit to the seven data points of Fig. 6, as explained above. This fit yields $\beta = 297(1)$ keV and $b = 98(1)$ keV and describes the experimental data fairly well (see Fig. 6). The value obtained for the relative strength β of the proton-neutron quadrupole interaction is quite insensitive to any reasonable parametrization of the unperturbed proton energies. Even when a fit is performed with the value of $b = 230(40)$ keV from Ref. [6], the resulting value for β decreases by about 4% only. In the case where the $B(M1)$-weighted average value for the energy of the $2_{1,\mathrm{ms}}^+$ state of ^{130}Te is included in the fitting procedure, the results are $\beta = 311(1)$ keV and $b = 96(1)$ keV. If we consider the energies of the main fragments of the MSS instead of the $B(M1)$-weighted average values, the results are $\beta = 306(1)$ keV and $b = 102(1)$ keV. Taking into account all these systematic deviations, we have adopted $\beta = 300(12)$ keV for the relative strength of the proton-neutron interaction in the $N = 78$ isotonic chain.

The value derived for the relative strength β of the proton-neutron quadrupole interaction in the $N = 78$ isotonic chain is about 14% smaller than that for the $N = 80$ isotopic chain [6] and about 6% smaller than the value for the xenon isotopic chain [8]. In contrast to the lighter xenon isotopes, where the experimental sensitivity for identification of weakly collective 2^+ states is limited up to 2.1–2.3 MeV, for the $N = 78$ isotonic chain this sensitivity is up to 2.5 MeV and, in the case of ^{134}Ba [21], it extends to even higher energies. Moreover, the summed $B(M1)$ strength remains constant at about 0.18–0.2 μ_N^2 (Fig. 5). These observations for the $N = 78$ isotones are at odds with the argument that the decrease in the relative proton-neutron interaction with increasing size of the valence space is caused by unobserved fragments of the MSS suggested in the case of stable xenon isotopes [8]. We stress that the fitting procedure used here is an exact analog of the one employed to describe the evolution of one-phonon 2_1^+ and $2_{1,\mathrm{ms}}^+$ states in the $N = 80$ isotonic chain [6]. Therefore, the difference between the relative strengths of the proton-neutron quadrupole interaction for the $N = 80$ and $N = 78$ isotonic chains clearly indicates a dependence which may be related to the occupancy of the $\nu h_{11/2}$ orbital. Microscopic calculations of the evolution of the fundamental $2_{1,\mathrm{ms}}^+$ state [10,27] of $N = 78$ isotones are needed before further conclusions can be drawn on this point.

IV. CONCLUSION

An inverse-kinematics Coulomb excitation experiment was performed to identify the $2_{1,\mathrm{ms}}^+$ MSS of ^{136}Ce. From measured $M1$ transition strengths, the 2_4^+ level was found to be the dominant fragment of the $2_{1,\mathrm{ms}}^+$ state. The fragmentation of the one-phonon MSS of ^{136}Ce is much smaller than the one observed in ^{138}Ce [5], demonstrating the importance of the neutron degree of freedom for understanding the origin and the generic nature of the mechanism of shell stabilization of MSS. The evolution of the one-phonon quadrupole collective states in the $N = 78$ isotonic chain yields a value for the proton-neutron quadrupole interaction slightly, but significantly, smaller than the ones derived for the $N = 80$ isotonic chain [6] and for the xenon isotopic chain [8]. However, the available experimental data on MSS in the $N = 78$ isotonic chain do not allow this decrease to be attributed to unobserved fragments of the MSS. Most likely, the differences between the relative strengths of the proton-neutron quadrupole interaction for $N = 80$ and $N = 78$ isotonic chains are related to the occupancy of the neutron $h_{11/2}$ orbital, an interpretation that requires validation through microscopic calculations.

ACKNOWLEDGMENTS

We thank the technical staff of the ATLAS facility at Argonne National Laboratory for its work in preparing and producing the ^{136}Ce beam for this experiment and R. V. Jolos for discussions. G.R. is a research fellow of the Alexander von Humboldt Foundation. This work was supported by the US Department of Energy, Office of Nuclear Physics, under Contracts No. DE-AC02-06CH11357 and No. DE-FG02-91ER40609, by the DFG under Grants No. Pi 393/2-2 and No. SFB 634, by the German-Bulgarian exchange program under Grant No. PPP 50751591, by the BgNSF under Grant No. DO 02-219, and by the Helmholtz International Center for FAIR.

[1] F. Iachello and A. Arima, *The Interacting Boson Model* (Cambridge University Press, Cambridge, 1987).
[2] F. Iachello, Phys. Rev. Lett. **53**, 1427 (1984).
[3] N. LoIudice and F. Palumbo, Phys. Rev. Lett. **41**, 1532 (1978).
[4] N. Pietralla, P. von Brentanto, and A. F. Lisetskiy, Prog. Part. Nucl. Phys. **60**, 225 (2008).

[5] G. Rainovski, N. Pietralla, T. Ahn, C. J. Lister, R. V. F. Janssens, M. P. Carpenter, S. Zhu, and C. J. Barton III, Phys. Rev. Lett. **96**, 122501 (2006).
[6] T. Ahn, L. Coquard, N. Pietralla, G. Rainovski, A. Costin, R. V. F. Janssens, C. J. Lister, M. P. Carpenter, S. Zhu, and K. Heyde, Phys. Lett. B **679**, 19 (2009).
[7] L. Coquard, N. Pietralla, T. Ahn, G. Rainovski, L. Bettermann, M. P. Carpenter, R. V. F. Janssens, J. Leske, C. J. Lister, O. Möller, W. Rother, V. Werner, and S. Zhu, Phys. Rev. C **80**, 061304 (2009).
[8] L. Coquard, N. Pietralla, G. Rainovski, T. Ahn, L. Bettermann, M. P. Carpenter, R. V. F. Janssens, J. Leske, C. J. Lister, O. Möller, W. Rother, V. Werner, and S. Zhu, Phys. Rev. C **82**, 024317 (2010).
[9] M. Danchev, G. Rainovski, N. Pietralla, A. Gargano, A. Covello, C. Baktash, J. R. Beene, C. R. Bingham, A. Galindo-Uribarri, K. A. Gladnishki, C. J. Gross, V. Y. Ponomarev, D. C. Radford, L. L. Riedinger, M. Scheck, A. E. Stuchbery, J. Wambach, C.-H. Yu, and N. V. Zamfir, Phys. Rev. C **84**, 061306 (2011).
[10] N. Lo Iudice, C. Stoyanov, and D. Tarpanov, Phys. Rev. C **77**, 044310 (2008).
[11] K. Sieja, G. Martínez-Pinedo, L. Coquard, and N. Pietralla, Phys. Rev. C **80**, 054311 (2009).
[12] K. Heyde and J. Sau, Phys. Rev. C **33**, 1050 (1986).
[13] T. Ahn, N. Pietralla, G. Rainovski, A. Costin, K. Dusling, T. C. Li, A. Linnemann, and S. Pontillo, Phys. Rev. C **75**, 014313 (2007).
[14] I.-Y. Lee, Nucl. Phys. A **520**, 641 (1990).
[15] P. Nolan, F. Beck, and D. Fossan, Annu. Rev. Nucl. Part. Sci. **45**, 561 (1994).
[16] A. A. Sonzogni, Nucl. Data Sheets **95**, 837 (2002).
[17] H. Ower, Ph.D. thesis, Johann-Wolfgang-Goethe-Universität zu Frankfurt am Main, 1980.
[18] A. Lell, Master's thesis, Universität München, 1978.
[19] A. Winther and J. de Boer, in *Coulomb Excitation*, edited by K. Alder and A. Winther (Academic Press Inc., New York, 1966) p. 303.
[20] K. Alder, A. Bohr, T. Huus, B. Mottelson, and A. Winther, Rev. Mod. Phys. **28**, 432 (1956).
[21] B. Fazekas, T. Belgya, G.Molnár, and Á. Veres, Nucl. Phys. A **548**, 249 (1992).
[22] N. Pietralla, D. Belic, P. von Brentano, C. Fransen, R.-D. Herzberg, U. Kneissl, H. Maser, P. Matschinsky, A. Nord, T. Otsuka, H. H. Pitz, V. Werner, and I. Wiedenhöver, Phys. Rev. C **58**, 796 (1998).
[23] E. Williams, R. J. Casperson, V. Werner, H. Ai, P. Boutachkov, M. Chamberlain, G. Gürdal, A. Heinz, E. A. McCutchan, J. Qian, and R. Winkler, Phys. Rev. C **80**, 054309 (2009).
[24] K. A. Gladnishki, G. Rainovski, P. Petkov, J. Jolie, N. Pietralla, A. Blazhev, A. Damyanova, M. Danchev, A. Dewald, C. Fransen, M. Hackstein, D. Karagyozov, O. Möller, T. Pissulla, M. Reese, W. Rother, and R. Topchiyska, Phys. Rev. C **82**, 037302 (2010).
[25] G. Molnár, R. A. Gatenby, and S. W. Yates, Phys. Rev. C **37**, 898 (1988).
[26] S. F. Hicks, J. R. Vanhoy, and S. W. Yates, Phys. Rev. C **78**, 054320 (2008).
[27] R. V. Jolos, N. Pietralla, N. Y. Shirikova, and V. V. Voronov, Phys. Rev. C **84**, 014315 (2011).